

Synthesis, structure and properties of a new phosphate $\text{Eu}_{1/3}\text{Zr}_2(\text{PO}_4)_3$

M. Alami and R. Brochu

Laboratoire de Chimie du Solide Appliquée, Avenue Ibn Batouta, Faculté des Sciences, Rabat (Morocco)

C. Parent, L. Rabardel, C. Delmas and G. Le Flem

Laboratoire de Chimie du Solide du CNRS, 351 cours de la Libération, 33405 Talence (France)

Abstract

A new phase $\text{Eu}_{1/3}\text{Zr}_2(\text{PO}_4)_3$ of Nasicon type structure was prepared via a sol–gel route. The crystallization process was investigated using Eu^{3+} as a structural probe. The decomposition of this phase at 900°C leads to a complex ceramic exhibiting a very low thermal expansion coefficient between room temperature and 1340°C : $\langle\alpha\rangle \approx 1 \times 10^{-7}^\circ\text{C}^{-1}$. Chemical intercalation of lithium gives rise to a new Eu^{2+} -rich phosphate $\text{Li}_x\text{Eu}_{1/3}\text{Zr}_2(\text{PO}_4)_3$ ($x \approx 0.33$).

1. Introduction

Nasicon type phosphates with general formula $\text{M}_x\text{M}_2(\text{PO}_4)_3$ have been extensively studied with respect to their exchange, catalytic and luminescent properties [1–3] as well as possible applications in various fields of material science as solid electrolytes [4], low thermal expansion ceramics [5–7] and matrices for waste storage [8]. In these phosphates M is usually a monovalent cation: alkali, copper, silver or a divalent cation (Ca^{2+} , Sr^{2+}). Two studies on the introduction of a rare earth in this structure type have been published [9, 10]. The present paper reports on a preliminary investigation of the new phosphate $\text{Eu}_{1/3}\text{Zr}_2(\text{PO}_4)_3$ obtained via a sol–gel route. The crystallization process was investigated by X-ray diffraction (XRD) as well as structural probing. The compound was also characterized by its dilatometric and intercalation properties.

2. Elaboration

The starting compounds, Eu_2O_3 and $\text{ZrOCl}_2 \cdot 8\text{H}_2\text{O}$ were dissolved separately in 2 N HNO_3 . The solutions were then mixed in stoichiometric proportions. The addition of a solution of $\text{NH}_4\text{H}_2\text{PO}_4$ under constant stirring produced a colourless gel. The gel and floating solution mixture were maintained for 24 h at 75°C and then progressively heated up to 400°C to allow both ammonia and nitrous vapours to evolve. The white powder obtained was amorphous. Crystallization begins at 750°C and is complete at 800°C after long annealing. Above 900°C $\text{Eu}_{1/3}\text{Zr}_2(\text{PO}_4)_3$ starts to decompose. Ultimately, at 1300°C , the following phases

can be detected by XRD: ZrP_2O_7 , EuPO_4 , $\text{Zr}_2\text{P}_2\text{O}_9$ and ZrO_2 .

3. Gel–crystal transition and structural investigation

The structural evolution during gel–crystal transition was continuously observed at various temperatures by recording the $^5\text{D}_0 \longrightarrow ^7\text{F}_J$ ($J = 0, 1, 2$) emission of Eu^{3+} . The emission spectrum of the gel dried at 75°C and more specifically the $^5\text{D}_0 \longrightarrow ^7\text{F}_0$ transition energy are identical with those of Eu^{3+} in nitric solution, indicating similar solvation of this ion in both media (Fig. 1).

At higher temperatures the Eu^{3+} emission changes strongly. Broadening of all the emission bands is observed as well as an increase in the intensity ratio:

$$R = \frac{I(^5\text{D}_0 \longrightarrow ^7\text{F}_2)}{I(^5\text{D}_0 \longrightarrow ^7\text{F}_1)}$$

For samples dried at 200°C , $R = 2.6$ and at 600°C , $R = 4.2$. These evolutions involve a continuum of low symmetrical sites for Eu^{3+} (Fig. 2).

The crystallization at 800°C corresponds to a narrowing of all the $^5\text{D}_0 \longrightarrow ^7\text{F}_J$ lines (Fig. 2). A unique $^5\text{D}_0 \longrightarrow ^5\text{F}_0$ line is observed at 17355 cm^{-1} ; with regard to the nephelauxetic scale [11] this rather high value is consistent with a weak crystal field acting at the rare earth site, *i.e.* with relatively large $\langle\text{Eu}-\text{O}\rangle$ distances compared with the value deduced from the ionic radii [12].

The framework of the structure is only produced at the end of the crystallization process and Eu^{3+} ions are located in a unique non-centrosymmetrical site.

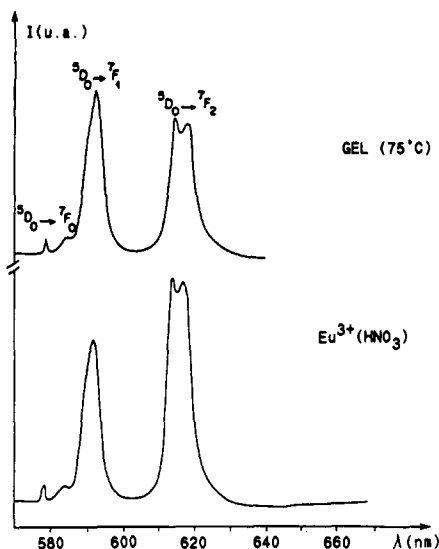


Fig. 1. Comparison of Eu^{3+} emission spectra in the investigated gel and in the nitric solution.

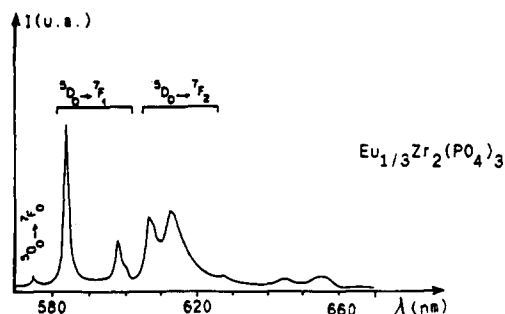
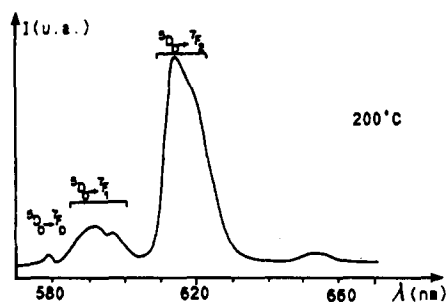
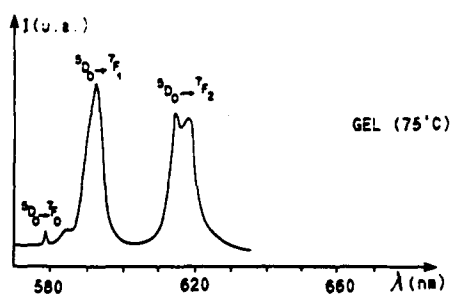


Fig. 2. Eu^{3+} emission spectra for the gel, the gel heated at 200°C and the crystalline phase $\text{Eu}_{1/3}\text{Zr}_2(\text{PO}_4)_3$.

TABLE 1. Comparison between the cell parameters of Nasicon-type phosphates

	$a(\text{\AA})$	$c(\text{\AA})$
$\text{NaZr}_2(\text{PO}_4)_3$ [13]	8.804	22.758
$\text{Ca}_{0.5}\text{Zr}_2(\text{PO}_4)_3$ [8]	8.800	22.60
$\text{Eu}_{1/3}\text{Zr}_2(\text{PO}_4)_3$	8.767	22.91

The XRD pattern of the crystallized sample can be indexed assuming a hexagonal cell: $a_h = 8.767 \pm 0.005 \text{ \AA}$, $c_h = 22.91 \pm 0.03 \text{ \AA}$ ($d_{\text{exp}} = 3.34$, $d_x = 3.293$). All the observed lines, except for two at low angles, are compatible with the $R3c$ space group: $7.56 \text{ \AA} - 5.70 \text{ \AA}$.

These results can be analysed within the scope of the crystallographic data of zirconium Nasicon-type phosphates containing ions with size comparable with that of Eu^{3+} (0.947 \AA [12]).

The spectral distribution of the $^5\text{D}_0 \rightarrow ^7\text{F}_j$ lines is compatible with the location of Eu^{3+} in the site usually labelled M_1 , an elongated antiprism sharing common faces with two ZrO_6 octahedra in a direction parallel to the c axis.

Table 1 compares the parameters of $\text{Eu}_{1/3}\text{Zr}_2(\text{PO}_4)_3$ with those of $\text{NaZr}_2(\text{PO}_4)_3$ ($R_{\text{Na}^+} = 1.02 \text{ \AA}$ [12]) and $\text{Ca}_{0.5}\text{Zr}_2(\text{PO}_4)_3$ ($R_{\text{Ca}^{2+}} = 1.00 \text{ \AA}$ [12]).

The rules governing the variation of the Nasicon type phosphate parameters have been reported previously [14]. The value of the c parameter results from the competition between the coulombic attraction of the cation in (M_1) with the surrounding oxygen atoms and the $\text{O}^{2-}\text{O}^{2-}$ repulsion occurring when M_1 is empty. Clearly the first factor prevails with substitution of Ca^{2+} for Na^+ . In contrast, the high c value of the europium phosphate is the consequence of the high vacancy concentration in the M_1 sites.

4. Preliminary investigation of the dilatometric and intercalation properties

Dilatometric measurements were performed between room temperature and 1347°C using a Netzch 402 ED3 differential dilatometer. The results are summarized in Figs. 3 and 4.

The thermal expansion of $\text{Eu}_{1/3}\text{Zr}_2(\text{PO}_4)_3$ is slightly positive ($\Delta L/L \approx 1.5 \times 10^{-3}$) until the beginning of decomposition at about 900°C which induces a marked shrinkage (Fig. 3). The resulting composite exhibits a remarkably weak thermal expansion coefficient ($\langle \alpha \rangle \approx 1 \times 10^{-7} \text{ }^\circ\text{C}^{-1}$) between room temperature and 1340°C (Fig. 4). A detailed study of this new complex ceramic is presently in progress.

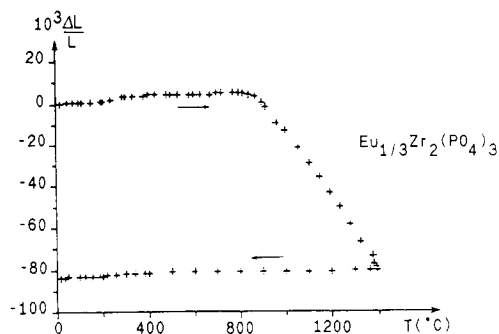


Fig. 3. Thermal expansion of $\text{Eu}_{1/3}\text{Zr}_2(\text{PO}_4)_3$ with increasing and decreasing temperature.

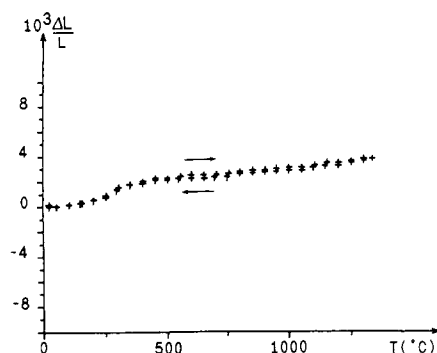


Fig. 4. Thermal expansion of the complex ceramic with increasing and decreasing temperature.

A large amount of lithium leads to the formation of a new phosphate with composition $\text{Li}_x\text{Eu}_{1/3}\text{Zr}_2(\text{PO}_4)_3$ ($x \approx 0.33$ from chemical analysis). The XRD pattern of this phase can be indexed assuming a hexagonal cell: $a = 8.75 \pm 0.005 \text{ \AA}$, $c = 23.17 \pm 0.003 \text{ \AA}$.

The intercalation process corresponds to the reduction of the majority of Eu^{3+} to Eu^{2+} . This can be checked (1) by the increase in the c parameter since the ionic radius of Eu^{2+} ($R = 1.17$ [12]) is larger than that of Eu^{3+} ($R = 0.95$), and (2) by the existence, under 300 nm excitation, of a broad band emission peaking at 460 nm and characteristic of Eu^{2+} (Fig. 5).

5. Conclusions

The new phosphate $\text{Eu}_{1/3}\text{Zr}_2(\text{PO}_4)_3$ exhibits interesting properties in very different fields of solid state chemistry and material science. These preliminary results need a more complete investigation from various viewpoints: ceramic sintering, intercalation mechanism and Eu^{2+} luminescence optimization.

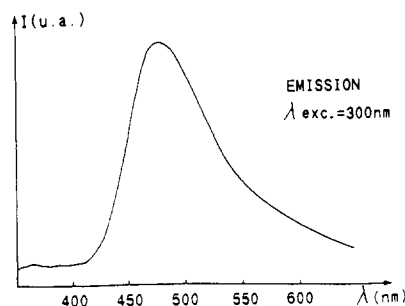
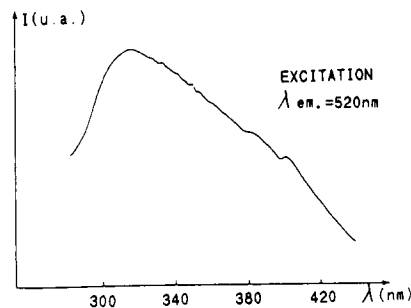


Fig. 5. Excitation and emission spectra of $\text{Li}_x\text{Eu}_{1/3}\text{Zr}_2(\text{PO}_4)_3$ ($x \approx 0.33$, $T = 300 \text{ K}$).

References

- 1 R. Brochu, A. Lamzibri, A. Addane, S. Arsalane and M. Ziyad, *Eur. J. Solid State, Inorg. Chem.*, 28 (1991) 253.
- 2 A. Serghini, R. Brochu, M. Ziyad, M. Loukah and J. C. Vedrine, *J. Chem. Soc. Faraday Trans.*, 87 (15) (1991) 2487.
- 3 G. Le Polles, C. Parent, R. Olazcuaga, G. Le Flem and P. Hagenmuller, *C. R. Acad. Sci. (Paris), Ser. II*, 306, (1988) 765.
- 4 J. B. Goodenough, H. Y. P. Hong and J. A. Kafalas, *Mater. Res. Bull.*, 11 (1976) 103.
- 5 R. Roy, D. K. Agrawal, J. Alamo and R. A. Roy, *Mater. Res. Bull.*, 19 (1984) 471.
- 6 S. Y. Li Maye, D. K. Agrawal and H. H. McKinstry, *J. Am. Ceram. Soc.*, 70 (10) (1987) C232.
- 7 T. Oota and I. Yamai, *J. Am. Ceram. Soc.*, 69 (1) (1986) 1.
- 8 R. Roy, E. R. Vance and J. Alamo, *Mater. Res. Bull.*, 17 (1982) 585.
- 9 R. Salmon, C. Parent, M. Vlasse and G. Le Flem, *Mater. Res. Bull.*, 14 (1979) 85.
- 10 S. Senbhagaraman and A. M. Umarji, *J. Solid State Chem.*, 85 (1990) 169.
- 11 P. Caro, O. Beury and E. Antic, *J. Phys. (Paris)* 37 (1976) 671.
- 12 R. D. Shannon, *Acta Crystallogr. A*, 32 (1976) 75.
- 13 L. O. Hagman and P. Kierkegaard, *Acta Chem. Scand.*, 22 (1968) 1822.
- 14 F. Cherkaoui, J. C. Viala, C. Delmas and P. Hagenmuller, *Solid State Ionics*, 21 (1986) 333.